Turbulence, Heat and Mass Transfer 5
K. Hanjaliæ, Y. Nagano and S. Jakirlic (Editors)

Effect of Transient Heat Transfer on Metal Particle Ignition

K. A. Avdeev[1], F. S. Frolov[2], S. M. Frolov[2], and B. Basara[3]
[1]*Tula State University,*
Tula, Russia
[2]*Semenov Institute of Chemical Physics,*
Moscow, Russia, smfrol@chph.ras.ru
[3]*AVL LIST GmbH*
Graz, Austria

Abstract - Ignition and combustion of metal particles are the issues of interest for many industrial and aerospace applications. When simulating ignition and combustion of metal particles using available standard models, a number of simplifying assumptions are usually adopted, which are not always justified. The objective of this work is to develop a new particle heating model with the correction factors to the Newton law taking into account transient heat transfer to a particle and nonuniform temperature distribution inside the particle. The new particle heating model was shown to correlate much better with detailed numerical calculations than the standard model. The transient heating effects were proved to be important for the problem of solid particle ignition in the oxidizer gas.

1. Introduction

Dynamics of heating, ignition, and combustion of reactive metal particles in turbulent flows are the issues important for various applications, including aerospace and chemical technologies, chemical propulsion, ground transportation, and industrial safety [1]. Modern CFD software packages utilize the simplest standard models of particle heating based on the Newton law [2] and particle ignition and combustion based on overall heterogeneous or homogeneous, Arrhenius-type, macrokinetic laws of several reactions [3].

The validity of many assumptions adopted in such standard models remains questionable. First, the Newton law is known to be valid only for steady-state heat transfer and the consequences of its application to intrinsically transient problems of particle heating and ignition are not quite clear. Second, the standard models deal with the mean particle temperature, thus assuming that the thermal conductivity of particle material is infinitely large. Third, application of convective heat transfer correlations of the Ranz–Marshall type [4] for modeling heat fluxes between solid particles and gas in two-phase turbulent flows is also not fundamentally substantiated. Such correlations were derived from the measurements in steady-state flows and their use in transient conditions is questionable. Regarding the overall kinetic law of particle ignition, it is usually derived by fitting the measured ignition delays and the results of calculations based on the standard particle ignition model with several unknown Arrhenius parameters (e.g., preexponential factor and activation energy) [5]. The Arrhenius parameters of the overall reaction rate constants are then found by applying the least-square procedure. In view of the above assumptions adopted in the standard model of particle heating, the Arrhenius parameters thus obtained can appear to have little common with the actual values relevant to the problem under consideration. There are many examples in the literature, when the values of preexponential factors and activation energies determined for particular conditions of particle ignition (e.g., large samples of cubic or cylindrical geometry, etc.) were applied for other

samples of cubic or cylindrical geometry, etc.) were applied for other conditions (fine particles of spherical or flaked shape, thin filaments, etc.). In view of these implications, there is a need in a reliable model of metal particle heating to provide the basis for improved modeling of particle ignition and combustion.
The objective of this work is to develop a new particle heating model with the correction factors to the Newton law taking into account transient heat transfer between a particle and the ambient gas and nonuniform temperature distribution inside the particle.

2. Formulation

2.1 Standard Model

The standard model (further referred to as the ST-model) of spherical particle heating in the quiescent gas is written in the form [1]:

$$cm\frac{d\overline{T}}{dt} = aS(T_{g\infty} - \overline{T}) \tag{1}$$

with the initial condition

$$\overline{T}(0) = T_0 \tag{2}$$

where t is time, $\overline{T}$ is the mean particle temperature, $T_{g\infty}$ is the ambient gas temperature, a is the heat transfer coefficient, $S = 4pR^2$ is the particle surface area, $m = (4/3)prR^3$ is the particle mass, c is the specific heat of particle material, r is the particle material density, and R is the particle radius. From now on, index 0 relates to the initial parameters, and index g relates to gas. The heat transfer coefficient a is determined from condition Nu = 2, i.e., $a = l_g / R$, where Nu is the Nusselt number and l is the thermal conductivity. Coefficient l_g is usually calculated at a certain reference temperature, e.g., $(\overline{T} + T_{g\infty})/2$.

Introducing the characteristic time scale of particle heating, R^2/a ($a = l/(r\,c)$ is the thermal diffusivity of particle material), and characteristic temperature, T_0, the standard model of Eqs. (1) and (2) can be presented in the dimensionless form:

$$\frac{d\overline{\Theta}}{d\mathrm{Fo}} = 3\,\mathrm{Bi}\left[\Theta_{g\infty} - \overline{\Theta}\right];\ \overline{\Theta}(0) = 1 \tag{3}$$

where $\overline{\Theta} = \overline{T}/T_0$ is the dimensionless mean particle temperature, $\Theta_{g\infty} = T_{g\infty}/T_0$ is the dimensionless gas temperature at a large distance from the particle, $\mathbf{Fo} = at/R^2$ is the Fourier number, and $\mathbf{Bi} = aR/l$ is the Biot number.

2.2 New Model

Generally speaking, the Newton law used in Eqs. (1) and (2) is valid only for the steady-state conditions. In transient conditions, the coefficient a will be a function of time, e.i., $a = a_{eff} = a\,(t)$. Moreover, Eq. (1) implies that the mean particle temperature $\overline{T}$ is equal to the particle

surface temperature T_i, which is not true, in particular at the initial stage of the particle heating process.
Thus, Eq. (1) should be replaced by equation:

$$cm\frac{d\overline{T}}{dt} = a_{eff} S(T_{g\infty} - T_i) \tag{4}$$

which is also subjected to the initial condition of Eq. (2). To complete the statement of the problem, one has to determine parameters a_{eff} and T_i as functions of time *t*, mean particle temperature $\overline{T}$, and thermophysical parameters of the problem. The new particle heating model based on Eq. (4) will be further referred to as the NEW-model.
In the dimensionless form, Eq. (4) can be written as:

$$\frac{d\overline{\Theta}}{d\mathrm{Fo}} = 3\,\mathrm{Bi}_{\mathrm{eff}} \left[\Theta_{g\infty} - \Theta_i\right];\ \overline{\Theta}(0) = 1 \tag{5}$$

where $\Theta_i = T_i / T_0$ is the dimensionless particle surface temperature and $\mathrm{Bi}_{\mathrm{eff}} = a_{eff} R / l$ is the effective Biot number.
The approximate relationship for the coefficient a_{eff} entering $\mathrm{Bi}_{\mathrm{eff}}$ can be obtained using the analytical solution of the transient heat transfer problem between a spherical particle and ambient gas at constant particle temperature ($\overline{T} = T_i$ = const) [6]:

$$a_{eff} \approx l_{eff} R^{-1} = l_g \left(1 + \sqrt{\frac{R^2}{p\, a_g\, t}}\right) R^{-1} \tag{6}$$

where $a_g = l_g / r_g c_p$ is the gas thermal diffusivity and c_p is the specific heat of gas at constant pressure. Equation (6) was obtained from the comparison of two relationships for the heat flux to/from the particle surface, namely, the Newton law,

$$q = a_{eff} (T_{g\infty} - T_i)$$

and the relationship derived from the analytical solution,

$$q = \frac{l_g \left(T_{g\infty} - T_i\right)}{R} \left(1 + \frac{R}{\sqrt{p\, a_g\, t}}\right)$$

To determine the dimensionless particle surface temperature Θ_i entering Eq. (5), the following approach was used. The temperature Θ_i was assumed to be a polynomial function of the mean particle temperature $\overline{\Theta}$:

$$\Theta_i = \sum_{j=0}^{n} b_j \overline{\Theta}^{\,j}; \tag{7}$$

where *n* is the polynomial order and b_j are the polynomial coefficients. To determine *n* and b_j, a detailed problem of particle heating described in the next subsection was formulated and solved.

2.3 Detailed Model

The detailed model of transient heat transfer between gas and a particle was formulated based on the following governing equations

$$\frac{\partial T_g}{\partial t} - a_g \frac{\partial^2 T_g}{\partial r^2} - \left(\frac{2a_g}{r} \right) \frac{\partial T_g}{\partial r} = 0 \tag{8}$$

$$\frac{\partial T}{\partial t} - a \frac{\partial^2 T}{\partial r^2} - \left(\frac{2a}{r} \right) \frac{\partial T}{\partial r} = 0 \tag{9}$$

subjected to the initial conditions:

$$t = 0 : \; T_g = T_{g\infty} ; \; T = T_0 \tag{10}$$

and boundary conditions:

$$r = 0 : \; \frac{\partial T}{\partial r} = 0 ; \; r = R : \; T = T_g = T_i , \; l \frac{\partial T}{\partial r} = l_g \frac{\partial T_g}{\partial r} ; \; r \to \infty : \; \frac{\partial T_g}{\partial r} = 0 \tag{11}$$

where r is the radial coordinate. The particle heating model based on Eqs. (8) and (9) and conditions (10) and (11) will be further referred to as the D-model.
In the dimensionless form, the D-model can be represented as:

$$b \frac{\partial \Theta_g}{\partial \mathrm{Fo}} - \frac{\partial^2 \Theta_g}{\partial x^2} - \frac{2}{x} \frac{\partial \Theta_g}{\partial x} = 0 ;$$

$$\frac{\partial \Theta}{\partial \mathrm{Fo}} - \frac{\partial^2 \Theta}{\partial x^2} - \frac{2}{x} \frac{\partial \Theta}{\partial x} = 0 \tag{12}$$

$$\mathrm{Fo} = 0 : \; \Theta_g = \Theta_{g\infty} ; \; \Theta = 1 \tag{13}$$

$$x = 0 : \; \frac{\partial \Theta}{\partial x} = 0 ; \; x = 1 : \Theta = \Theta_g = \Theta_i , \; \frac{\partial \Theta}{\partial x} = d \frac{\partial \Theta_g}{\partial x} ; \; x \to \infty : \frac{\partial \Theta_g}{\partial x} = 0 \tag{14}$$

where $b = a / a_g$ and $d = l_g / l$.

The set of Eqs. (12) with the initial and boundary conditions of Eqs. (13) and (14) was solved numerically using the implicit finite-difference scheme and the procedure described in [7]. The values of b_j in Eq. (7) were determined by statistical processing of numerical solutions for spherical particles of glass, steel, and silver 70 mm in diameter at different initial conditions (see Table 1). The calculations indicated that the polynomial of the third order (n = 3) was sufficient for attaining a reasonable agreement of Eq. (7) with the results of numerical solution. For example, for glass, steel, and silver particles heated in air at normal pressure, the error of the polynomial approximation of Eq. (7) did not exceed $e_{\max} \approx$ 0.5%–2.6% up to mean particle temperatures of $\overline{\Theta} = 4.3$ ($\overline{T} \approx 1250.15$ K). The error e was defined as

$$e = \left(1 - \frac{\overline{\Theta}}{\overline{\Theta}_D} \right) \cdot 100\% \tag{15}$$

where index D relates to the D-model. The recommended values of b_j are presented in Table 1.

Table 1: Recommended values of n and b_j in polynomial (7)

n	b_0	b_1	b_2	b_3
3	0.0469521	0.931	0.03682	–6.129e-3

3. Detailed Model Validation

The D-model was validated against the analytical solution for a spherical particle placed in the medium with constant temperature [8]. The analytical solutions for the particle surface ($x = 1$) and center ($x = 0$) temperatures are given by the function:

$$\Theta(x, \mathrm{Fo}) = 1 + \left\{1 - \sum_{\mathrm{n}=1}^{\infty}\left[A_n \frac{\sin x}{x m_{\mathrm{n}}} \cdot e^{-m_{\mathrm{n}}^2 \cdot \mathrm{Fo}}\right]\right\}\left(\Theta_{g\infty} - 1\right) \tag{16}$$

The analytical solution for the mean particle temperature is given by:

$$\overline{\Theta}(\mathrm{Fo}) = 3\int_0^1 x^2 \Theta(x, \mathrm{Fo})dx = 1 + \left\{1 - \sum_{\mathrm{n}=1}^{\infty}\left[\frac{3\mathrm{Bi}^2}{\left(m_{\mathrm{n}}^2 + \mathrm{Bi}^2 - \mathrm{Bi}\right) m_{\mathrm{n}}^2} e^{-m_{\mathrm{n}}^2 \cdot \mathrm{Fo}}\right]\right\}\left(\Theta_{g\infty} - 1\right) \tag{17}$$

where m_n are the roots of equation

$$\mathrm{tg} m_{\mathrm{n}} = -\frac{\mu_{\mathrm{n}}}{\mathrm{Bi} - 1}$$

and $A_n = \dfrac{2\left(\sin m_{\mathrm{n}} - m_{\mathrm{n}} \cos m_{\mathrm{n}}\right)}{m_{\mathrm{n}} - \sin m_{\mathrm{n}} \cos m_{\mathrm{n}}}$ is the coefficient.

Table 2 shows the maximal errors $e_{\max}$ of numerical calculations of $\overline{\Theta}$, Θ_i, and Θ_c (index c stands for particle center) for 70-micrometer-diameter glass and steel particles in relation to the analytical solutions of Eqs. (16) and (17). In addition, Table 2 shows the values of dimensionless time $\mathrm{Fo}_{e\,\max}$ to identify the conditions, when $e = e_{\max}$. Clearly, the maximal errors are attained at higher gas temperatures and do not exceed 0.6% when the computational grid in the particle contains N = 70 nodes. As could be expected, the error decreases with the number of computational nodes in the particle, resulting however in the growing CPU time.

Table 2: Maximal errors of numerical calculation of mean, surface, and center temperatures of spherical 70-micrometer-diameter glass and steel particles depending on the number of computational cells per particle N and dimensionless gas temperature $\Theta_{g\infty}$

Particle material	$\Theta_{g\infty}$	$\overline{\Theta}$		Θ_i		Θ_c	
		$e_{\max}$, %	$\mathrm{Fo}_{e\,\max}$	$e_{\max}$,%	$\mathrm{Fo}_{e\,\max}$	$e_{\max}$, %	$\mathrm{Fo}_{e\,\max}$
Glass N = 70	1.2388	0.064	7.475	0.066	7.200	0.063	8.150
	3.6607	0.544	1.725	0.532	1.825	0.588	1.725
Glass N = 700	3.6607	0.056	1.902	0.055	1.815	0.060	1.788
Steel N = 70	1.2388	0.042	200	0.041	200.0	0.042	200.0
	4.3089	0.302	103	0.303	103.0	0.301	103.0

To take into account thermal expansion of particle material due to transient particle heating, Eqs. (12) were also integrated with regard for the dependence of the material density on temperature. For steel particles, the arising difference in the calculated particle surface tempera-

tures was as low as 0.15% at a computational grid with $N = 70$. This error is well within the numerical errors of Table 2. Therefore, to simplify the calculations, thermal expansion of the materials was neglected.

4. Results Of Calculations

To study the comparative performance of the models described above, a set of calculations was made. Table 3 shows the list of particle materials analyzed, as well as relevant thermophysical properties used in the calculations. In all cases, the particle diameter was taken equal to 70 mm. In the calculations, temporal variation of particle mean temperature $\overline{\Theta}$ in hot air with temperature $\Theta_{g\infty}$ at atmospheric pressure was monitored. Table 4 and Figs. 1 to 3 show the results of calculations in terms of the maximal discrepancy, $e_{\max}$, of $\overline{\Theta}$ from the mean temperature predicted by the D-model, $\overline{\Theta}_{CJ}$, and the mean temperature itself predicted by

Table 3: Thermophysical properties of particle material

Particle material	l, W/(m· K)	c, J/(kg· K)	r, kg/m^3
Glass (at 293.15 K)	0.744	670.0	2500
Steel (at 293.15 K)	45.0	461.0	7900
Silver (at 273.15 K)	458.0	234.0	10500
Mercury (at 273.15 K)	7.9	138.0	13600

Table 4: Results of calculations for glass, steel, silver, and mercury particles at $\overline{\Theta}(0) = 1$ ($T_0 = 293.15$ K)

Particle material	$\Theta_{g\infty}$, (T_{g_∞}, K)	$e_{\max}$, %		$\overline{T}$, K	
		NEW	ST	NEW/D	ST/D
Glass	1.2388 (363.15)	0.473	– 0.564	360.79/362.50	334.79/332.91
	2.2622 (663.15)	– 1.120	– 7.100	341.93/338.19	462.01/431.38
	3.2855 (963.15)	– 1.790	– 15.320	320.76/315.14	552.37/478.96
	3.6607 (1073.15)	– 2.015	– 18.340	315.64/309.43	589.84/498.37
Steel	1.2388 (363.15)	– 0.069	– 0.380	307.48/307.26	315.64/314.45
	2.2622 (663.15)	– 0.580	– 7.200	363.81/361.71	451.18/420.87
	3.2855 (963.15)	– 0.574	– 15.700	329.70/327.92	561.38/485.20
	4.3089 (1263.15)	– 2.014	– 23.730	706.85/721.37	645.01/521.30
Silver	1.2388 (363.15)	– 0.044	0.045	295.96/295.83	294.30/294.43
	2.2622 (663.15)	– 0.460	– 1.450	308.69/307.28	311.72/307.28
	3.2855 (963.15)	– 0.740	– 4.890	321.78/319.42	335.03/319.42
	4.2066 (1233.15)	– 0.800	– 9.140	328.00/325.39	361.52/331.24
Mercury	1.2388 (363.15)	0.264	– 0.473	354.24/355.18	335.52/333.95
	1.5799 (463.15)	– 0.600	– 2.150	365.54/363.37	380.37/372.38
	1.9210 (563.15)	– 0.870	– 4.470	394.75/391.36	419.94/401.95
	2.2622 (663.15)	– 0.980	– 7.129	401.28/397.37	457.80/427.34

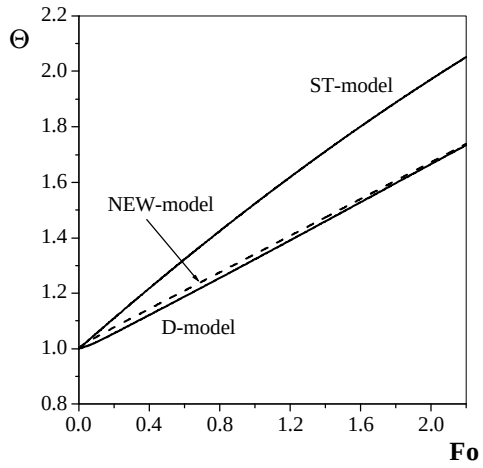

Figure 1: Time history of the mean temperature of a glass particle at T_{g_∞} = 1073 K

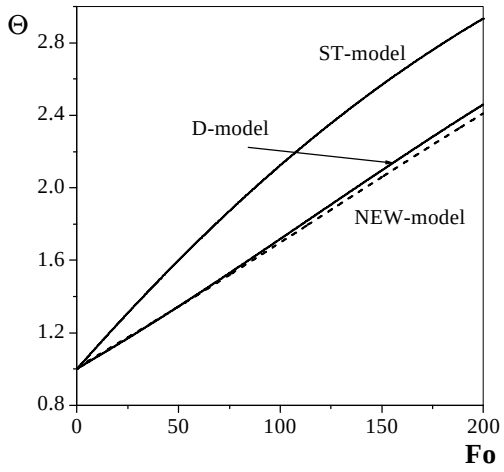

Figure 2: Time history of the mean temperature of a steel particle at T_{g_∞} = 1263 K

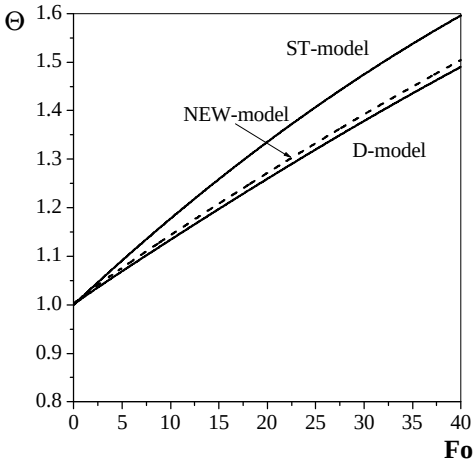

Figure 3: Time history of the mean temperature of a mercury particle at T_{g_∞} = 663 K

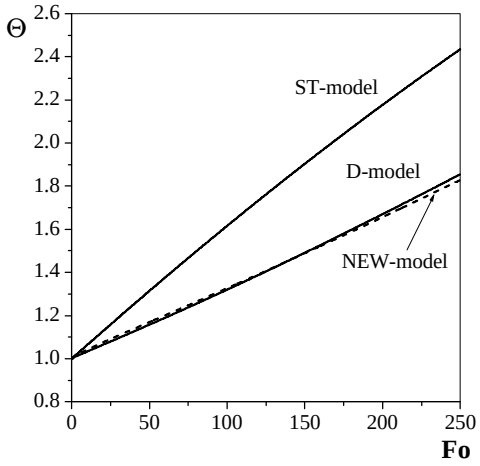

Figure 4: Time history of the mean temperature of a magnesium particle at T_{g_∞} = 1600 K

ST-, NEW- and D-models. For the sake of convenience, Table 4 shows the dimensional values of the corresponding temperatures. It is seen from Table 4 and Figs. 1 to 3 that contrary to the ST-model, the NEW-model correlates well with the D-model.

4. MODEL APPLICATION

To demonstrate the generality of the NEW-model, it was applied to the problem of aluminum, magnesium and boron particles heating in hot air at atmospheric pressure. Particles of these materials are widely used as energetic additives to propellants. Table 5 shows the corresponding thermophysical properties of these materials. Table 6 and Figs. 4 to 6 show the results of calculations at different air temperatures. The initial particle diameter was taken equal to 70 mm.

Table 5: Thermophysical properties of aluminum, magnesium, and boron at T_0 = 293.15 K

Particle material	l , W/(m· K)	c, J/(kg· K)	r , kg/m^3
Aluminum	225.0	900.0	2700
Magnesium	139.0	1020.0	1740
Boron (cristal.)	27.0	1026.0	2340

Table 6: Results of calculations for magnesium, aluminum, and boron particles at $\overline{\Theta}(0) = 1$ (T_0 = 293.15 K)

Particle material	$T_¥$, K	$e_{\max}$, %		`T, K	
		NEW	ST	NEW/D	ST/D
Magnesium	930.15	– 1.04	– 12.43	363.00/359.77	446.30/397.00
	1600.15	1.42	– 31.25	536.18/543.89	713.87/543.89
Aluminum	930.15	– 0.98	– 12.80	371.25/368.44	440.18/391.93
	1600.15	2.01	– 31.37	529.35/540.19	709.63/540.19
Boron	930.15	– 0.79	– 13.65	347.48/344.75	475.22/418.14
	1600.15	2.63	– 31.36	592.95/608.97	727.68/553.95

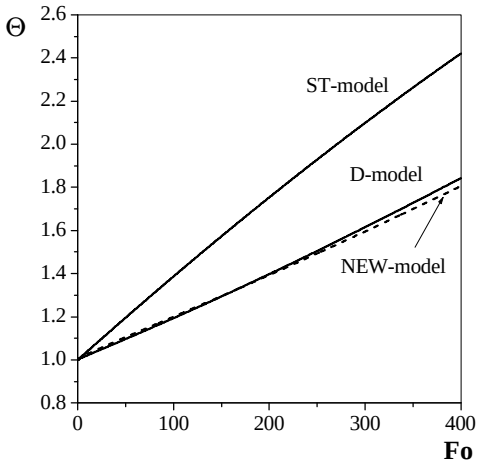

Figure 5: Time history of the mean temperature of aluminum particle at T_{g_∞} = 1600 K

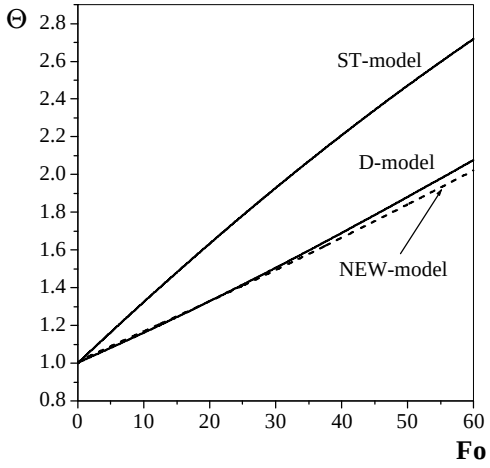

Figure 6: Time history of the mean temperature of boron particle at T_{g_∞} = 1600 K

Comparison between the D, ST, and NEW models indicates that the NEW-model correlates much better with the D model than the ST model. The maximal error in the predicted mean temperature inherent in the NEW model is only 1%–3%, while the error of the ST model reaches the value of up to 30%. The maximal error is attained at high gas temperatures.

6. Discussion

The results of calculations provide important implications for the problem of metal particle ignition in the oxidizing atmosphere. For example, the standard model often used in relevant studies of particle ignition predicts that the mean temperature of boron particle 70 mm in diameter attains a mean temperature of 727.68 K at 5.5 ms (Fo = 50.4), when it is placed in hot air with a temperature of 1600.15 K (see Fig. 6). This temperature (728 K) exceeds the melting temperature of the boron oxide film (≈723 K), which is often used as a critical temperature

of boron particle ignition. According to the NEW-model, during the time of 5.5 ms the boron particle heats only up to 542 K, other conditions being equal. This mean temperature value correlates well with the prediction provided by the D-model. Clearly, the arising difference in the mean temperature (about 185 K !) can exert a pronounced effect on the particle ignition timing.

The other important implication of the results is as follows. The macrokinetic Arrhenius parameters of the reaction rate constant relevant to metal particle ignition are often obtained based on fitting the experimental measurements of the particle ignition delay with the standard model similar to the model of Eq. (3) supplemented with the corresponding chemical source term. In view of the significant error associated with the use of the standard heating model, the corresponding Arrhenius parameters obtained by the least-square method could be incorrect. In any case, their applicability to the problems of ignition of particles possessing different size and shape should be properly substantiated.

An important advantage of the NEW-model is that it incorporates a particle surface temperature T_i, which can differ from the mean particle temperature. When solving the problem of particle ignition, this issue can manifest itself in the modification of the particle ignition timing, as the surface reaction rates are very sensitive to temperature.

Concluding Remarks

The dynamics of metal particle heating in a hot quiescent air was calculated using three models: (1) detailed model based on the conjugate equations of thermal conductivity in gas and particle, (2) approximate standard model based on the ordinary differential equation for mean particle temperature and the Newton law, and (3) new approximate model, based on the ordinary differential equation for the mean particle temperature and the Newton law applying the effective heat transfer coefficient and the particle surface temperature. The approximate dependence of the effective heat transfer coefficient on governing parameters and time was derived from the analytical solution for a particle with constant surface temperature. The dependence of the particle surface temperature on its mean temperature was found by generalizing the results of numerical solution of the conjugate problem.

Comparison of the computational results provided by the three models for glass, steel, silver, mercury, aluminum, magnesium, and boron particles showed that the new model correlates much better with the detailed model than the standard model. The maximal deviations of the predicted mean particle temperature from the solution of the detailed conjugate problem were less than 1%–2% for the new model and up to 30% for the standard model. The largest deviations were obtained for high air temperatures. The latter is particularly important for the problem of metal particle ignition in oxidizer gas. The other important advantage of the new model is that it contains the particle surface temperature, which differs from the particle mean temperature. When solving a problem of particle ignition, the use of the particle surface temperature may affect the process evolution in view of the strong dependence of the rate of heterogeneous reactions on temperature. This implication has been demonstrated on the example of boron particle ignition.

Acknowledgements

This work was supported by the Russian Foundation for Basic Research (grants 05-08-18200a and 05-08-50115a) and AVL LIST GmbH.

References

1. B. I. Khaikin, V. I. Bloshenko and A. G. Merzhanov. *Combustion, Explosion, and Shock Waves*, 4: 474–488, 1970.
2. F. Mashayek and R. V. R. Pandya. *Progr. Energy Combust. Sci.*, 29: 329, 2003.
3. J. F. Widener, Y. Liang and M. W. Beckstead. AIAA Paper 99-2629, 1999.
4. W. E. Ranz and W. R. Marshall. *Chem. Eng. Prog.*, 48: 141, 1952.
5. H. V. Cassel and I. Liebman. *Comb. Flame*, 7(1) , 1963.
6. S. S. Sazhin, V. A. Gol'dshtein and M. R. Heikal. *J. Heat Mass Transfer*, 123: 63–64, 2001.
7. S. M. Frolov, V. S. Posvianskii, V. Ya. Basevich, *et al*. *Rus J. Chemical Physics*, 23(1): 62–82, 2004.
8. A. V. Lyikov. *The theory of thermal conductivity*. Moscow: Vysshaya Shkola Publ., 1967.